# Journal of Materials Chemistry A

Accepted Manuscript


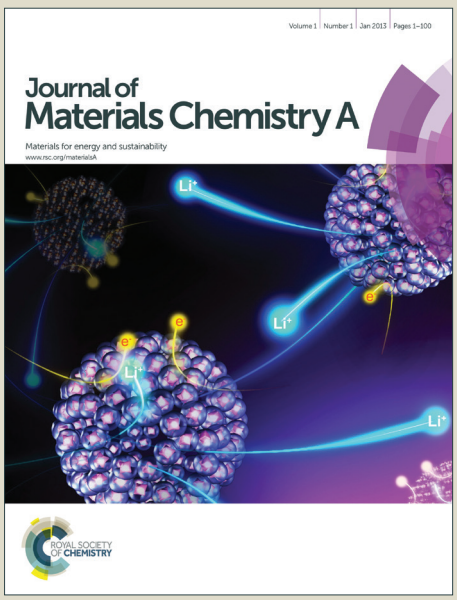





ROYAL SOCIETY OF CHEMISTRY

www.rsc.org/materialsA

Journal of Materials Chemistry A RSCPublishing

ARTICLE

# Enhanced electrochemical properties of $LiNiO_2$-based cathode material by removing lithium residues with $(NH_4)_2HPO_4$

Cite this: DOI: 10.1039/x0xx00000x

Xunhui Xiong,[a,b,1] Dong Ding,[b,1] Yunfei Bu,[b] Zhixing Wang,[*a] Bin Huang,[a] Huajun Guo[a] and Xinhai Li[a]

Received 00th January 2012,
Accepted 00th January 2012

DOI: 10.1039/x0xx00000x

www.rsc.org/

The lithium residues on surface of $LiNi_{0.8}Co_{0.1}Mn_{0.1}O_2$ have been removed by added $(NH_4)_2HPO_4$ in the solvent of ethanol. Different amount of $(NH_4)_2HPO_4$ are used to precipitate the inestimable lithium residues and the performances of respective $LiNi_{0.8}Co_{0.1}Mn_{0.1}O_2$ cathode materials show amazing differences. Under the optimized condition, the modified materials exhibit enhanced cycling performance, although XRD and TEM results demonstrate that the precipitated $Li_3PO_4$ is not coated on surface of $LiNi_{0.8}Co_{0.1}Mn_{0.1}O_2$. The capacity of the modified material exhibits 66.9% retention after 100 cycles at 2*C*, while the pristine material shows only 48.1% retention. The results demonstrate the removal of lithium residues on surface of $LiNiO_2$-based materials is effective in decreasing the side reactions. This property will be valuable for the option of coating methods and coating materials because the enhancement of coating will be maximized if the lithium residue can be removed after coating.

## Introduction

Recently, $LiNiO_2$-based cathode materials (Ni content<60%) for Li-ion batteries have been successfully commercialized as a result of intensive research and designed efforts. Further research to increase Ni content to >60% is being carried out to increase the energy density of Li-ion cells. Ni-rich (Ni content≥0.8) layered materials have been considered as promising candidates for hybrid electric vehicles, plug-in hybrid vehicles and electric vehicles due to their large capacity, excellent rate capability and low cost.[1-3] However, the rapid moisture uptaking ability of Ni-rich materials stemmed from the slow and spontaneous reduction of $Ni^{3+}$ and chemical/physical adsorptions of synthetic residue $Li_2O$/LiOH on surface has become one of the greatest technical hurdles for commercial application.[4-8] This problem results in gelation of the cathode slurry, which will cause irregular cathode coating thickness on Al foil. On the other hand, Ni-rich layered materials exhibit severely poor cycling performance, especially at elevated temperature and high voltage due to the reactive and unstable $Ni^{4+}$ ions in the delithiated materials.[9-15] Surface coatings of Ni-rich materials by $Al_2O_3$, MgO, $TiO_2$ and $SiO_x$ become effective ways to solve poor cycling problems. At the same time, these coating layers will isolate the materials from air, thus reduction of $Ni^{3+}$ is prevented.[11,16] However, as indicated by lots of reports, excess lithium is necessary for Ni-rich layered materials during annealing to get the best performance and the excess lithium ions do not occupy the transition metal sites.[4, 17-18] They will adhere on surface as $Li_2O$/LiOH and are expected to be still on surfaces of the particle after coating because they will not react with the coating layers during annealing.[10,13,19]

R. Moshtev et al. have summarized that LiOH in water originated basically from the chemical delithiation of $LiNiO_2$ phase when immersed in water. However, when $LiNiO_2$ were immersed in ethanol, the LiOH found in ethanol was mostly from the excess LiOH on surface, because the chemical delithiation was negligible due to kinetic hindrance,[20] which agrees with our previous results.[13] Based on this, ethanol is used as the solvent to dissolve the synthetic residues $Li_2O$/LiOH on the surfaces of Ni-rich materials in our study. After the synthetic residues are transferred to solvent from the surface of Ni-rich materials, $(NH_4)_2HPO_4$ is added to precipitate lithium residues $Li_2O$/LiOH. The effects and the mechanism of lithium residues and phosphate processing on the electrochemical performance and storage characteristic of $LiNiO_2$-based materials have never been reported.

## Experimental section

### Synthesis and characterization

$LiNi_{0.8}Co_{0.1}Mn_{0.1}O_2$ (NCM for short) was taken as an example from Ni-rich layered materials and was prepared by mixing co-precipitated $Ni_{0.8}Co_{0.1}Mn_{0.1}(OH)_2$ and $LiOH{\cdot}H_2O$ at a molar ratio of 1:1.05, and fired at 480 and 750°C in $O_2$ flow for 5 and 15h, respectively. In order to prepare $Li_3PO_4$-modified NCM, different amount of $(NH_4)_2HPO_4$ is dispersed in 200 g ethanol (≥98%) by continuous stirring and ultrasonic treatment followed by adding 100 g NCM. The suspension was constantly stirred for 5 h with a slow evaporation of ethanol. The obtained product was calcined at as low as 400°C to avoid the formation of $P_2O_5$.[21]

The crystal structure of the products was confirmed by X-ray powder diffraction (XRD, Rint-2000, Rigaku) using Cu-Kα radiation (1.54056Å). The morphology of the particles was measured by scanning electron microscope (JEOL, JSM-5612LV) with an accelerating voltage of 20 kV, and by transmission electron microscope (Tecnai G12, 200 kV). X-ray photoelectron spectroscopy (XPS, PHI 5600, Perkin-Elmer)

measurements were performed to get information on the surface of phosphate processed NCM.

For HF titration, ten cycled cells were carefully disassembled and all contents of the cell were washed thoroughly with DMC for one week in the glovebox. 0.01 mol·L$^{-1}$ NaOH aqueous solution and Bromothymol Blue (BTB, Aldrich) as an indicating solution were used for the titration of the extensively cycled electrolyte.

**Electrochemical measurement**

Electrochemical charge-discharge tests were performed using the cathode with a mixture of 80 wt.% cathode material, 10 wt.% Super P carbon black and 10 wt.% polyvinylidene fluoride (PVDF). The electrolyte was 1.0 M LiPF6/EC+DMC+EMC (1:1:1, volume ratio). Typical loading of the electrode material is 12 mg·cm$^{-2}$. Preliminary cell tests were done using 2025 coin-type cell adopting Li metal as an anode. The half-cells were first cycled for one cycle at a rate of 0.1C rate (1*C*= 18 mA·g$^{-1}$), followed by 0.5 and 2C for one cycle and 100 cycles, respectively, between 2.8~4.3 V at 25°C. The electrochemical impedance spectra (EIS) of the cells at 100% state of charge (SOC) after different cycles were measured over a frequency range from 100 kHz to 0.01 Hz in two-electrode cell.

## Results and discussion

In order to confirm the possible formation of $Li_3PO_4$ in ethanol, 0.01 mol $(NH_4)_2HPO_4$ and 0.03 mol $LiOH·H_2O$ were dispersed in 20 ml ethanol (≥98%) by continuous stirring and ultrasonic treatment. After dried at 80°C, the powder shows low crystallinity (exhibited in Fig.1(a)) and pure phase $Li_3PO_4$ after fired at 400°C. The results indicate that $Li_3PO_4$ will form in ethanol.

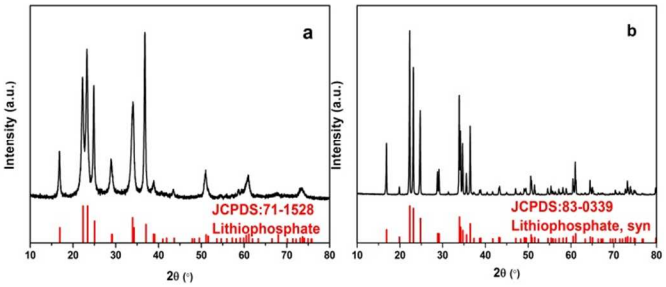


Fig.1 XRD patterns of $Li_3PO_4$ before calcined (a) and after calcined (b).

Owing to immeasurable amount of lithium residues, we first optimize the amount of required $(NH_4)_2HPO_4$ through electrochemical performance. The amount of lithium residues is estimated through pH value of NCM. The pH measurement of the powder is monitored by adding 100 g powders to 1000 mL purified water with constant stirring.[13] Assuming the pH value (pH=12.8) is contributed by lithium residues on surface completely and no chemical delithiation from bulk, then 0.06 mol LiOH adheres on the surfaces of the particles. Based on this assumption, 0.02 mol, 0.01 mol, 0.005 mol, 0 mol $(NH_4)_2HPO_4$ are dispersed in ethanol and used to precipitate lithium residues of 100 g NCM powders, respectively. The chemical reaction occurring in the system can be concluded as follows:

$$(NH_4)_2HPO_4+LiOH\rightarrow NH_3\uparrow+H_2O+Li_3PO_4 \quad (1)$$

After dried and calcined at 400°C, all samples are evaluated through electrochemical performance. The initial charge-discharge curves at 0.1*C* and cycle performance at 2*C* are shown in Fig.2, all samples show poor cycle performances, which are ascribed to the reactive and unstable $Ni^{4+}$ ions in the delithiated materials.[9-15] Additionally, NCM powders present significantly different performances after processed with various amounts of $(NH_4)_2HPO_4$. Excessive $PO_4^{3-}$ may capture lithium in the crystal lattice of NCM during the subsequently annealing process and destroy the materials.[22] NCM modified by 0.005 mol $(NH_4)_2HPO_4$ displays the best cycle performance, and the reason is unclear now. For the sake of precluding the potential effect of ethanol, powders processed with ethanol but no $PO_4^{3-}$ are also studied. They exhibit identically performances with pristine powders, which had been corroborated by R. Moshtev.[20] NCM with the most prominent performance (shown in Fig.2) is discussed in the following.

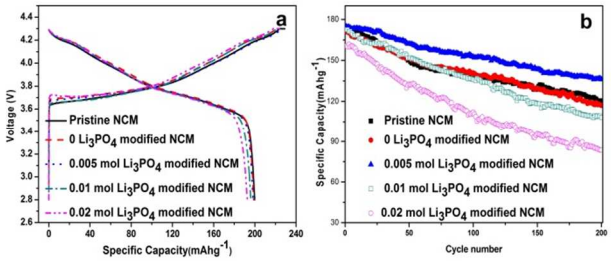


Fig.2 The initial charge-discharge curves at 0.1*C* (a) and cycling performance at 2*C* (b) of pristine NCM and samples after different amounts of $(NH_4)_2HPO_4$ processed.

Fig.3 shows the SEM and TEM images of the pristine NCM and NCM modified by 0.005 mol $(NH_4)_2HPO_4$. It is clear that there is no significant difference between the pristine and $Li_3PO_4$-modified NCM, and the surface of them are clean. The $Li_3PO_4$ are expected to precipitate on surface of NCM and form coating layer at the same time. However, TEM and HRTEM images also still show both of them have very smooth surfaces and they all show good crystallinity at the edges of the grains as well as no extra surface film. The precipitated $Li_3PO_4$ may nucleate seperately and just mix with NCM rather than coated on the surface of NCM. For the sake of further confirming the above phenomena, XRD and Rietveld refinements were conducted to analyse structure changes of the $Li_3PO_4$-modified NCM. As shown in Fig.4, the results reveal that all peaks could be an indexed hexagonal a-$NaFeO_2$ structure with a space group of $R\bar{3}m$. The lattice constants for pristine NCM ($a$=2.87198 Å, $c$=14.20706 Å) and $Li_3PO_4$-modified NCM ($a$=2.87183 Å, $c$= 14.20679 Å) estimated by Rietveld refinement imply that there is no significant difference in the crystal structure of NCM due to the low quantity and annealing temperature.

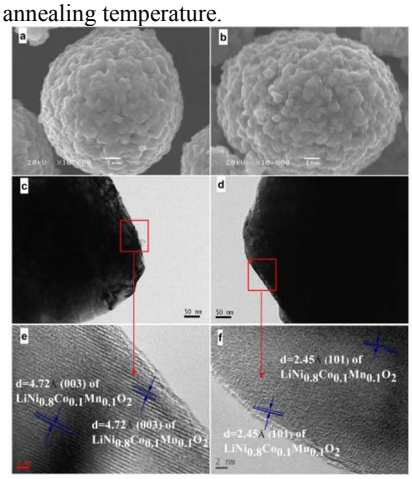


Fig.3 Typical SEM and TEM images of pristine (a), (c), (e) and $Li_3PO_4$-modified NCM (b), (d), (f).

EDX was performed to check the distribution of elements on the surface of $Li_3PO_4$-modified NCM. As shown in Fig.5, P element is detected in $Li_3PO_4$-modified NCM. From the elemental mapping

images, all elements are distributed uniformly except P. The P distribution of $Li_3PO_4$-modified sample shows large difference with that of coated sample and $Li_3PO_4$ is hardly addressed as coating layer when combined with the results of TEM images. As an effective method that can provide an elemental analysis of the surface film, XPS analysis of the $Li_3PO_4$-modified NCM was carried out and given in Fig.6. The peak of P 2p (133.5 eV) is seen in the modified compounds, which is characteristic of the tetrahedral ($PO_4$)-group.[23] It clearly reveals that the $Li_3PO_4$-modified NCM has Mn2p, Co2p and Ni2p peaks with negligible chemical shift of binding energy, indicating that the ion environments have no changes in the surface structure. However, a greater chemical shift for Li 1s and O 1s in Fig.6, indicates that the Li and O ion environment in the structure are changed by some chemical bond. One possibility is the existence of $Li_3PO_4$ phase in NCM.

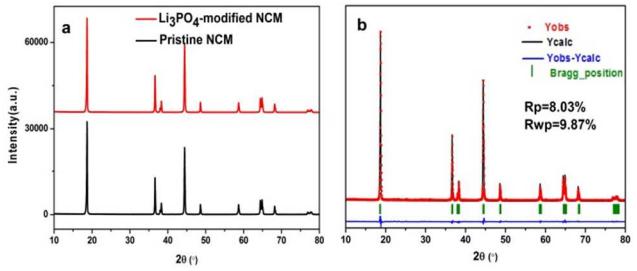


Fig.4 The XRD patterns (a) and Rietveld refinements (b) of pristine and $Li_3PO_4$-modified NCM.

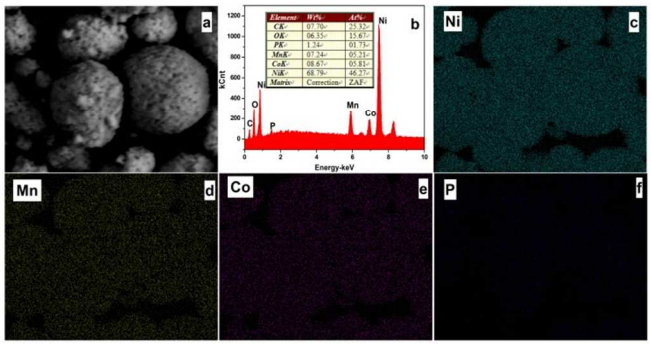


Fig.5 BSE micrographs (a), EDAX of $Li_3PO_4$-modified NCM (b) and elemental maps for Ni (c), Mn (d), Co (e) and P (f) for the same region, obtained by EDX mapping.

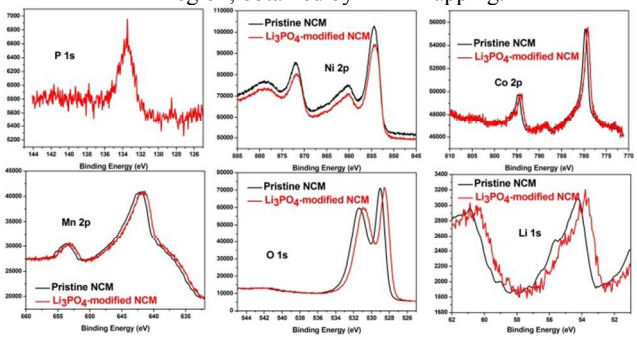


Fig.6 XPS spectra of pristine NCM and $Li_3PO_4$-modified NCM.

Fig.7(a) exhibits the cycle performance of pristine and $Li_3PO_4$-modified NCM at 2*C* at 60°C. Compared with the cycle performance at room temperature (shown in Fig.1), the improvement at 60°C is more significant. The capacity of pristine material fades rapidly from 174.1 mAh·g$^{-1}$ for the first cycle to 83.8 mAh·g$^{-1}$ for the 100$^{th}$ cycle, or only 48.1% retention after 100 cycles. However, the $Li_3PO_4$-modified NCM demonstrates much more improved capacity retention, which is about 66.9% of the initial capacity after 100 cycles. The discharge curves of the first cycle and 100$^{th}$ cycle at 2*C* rate are shown in Fig.7(b). The $Li_3PO_4$-modified NCM displays a similar polarization at the first cycle. After 100 cycles, the pristine electrode shows a much higher polarization. These poor cycling performances of the pristine NCM is attributed to its vigorous surface reactivity with liquid electrolyte, and the reason for $Li_3PO_4$-modified NCM is unclear because of no extra coating layer on surface.

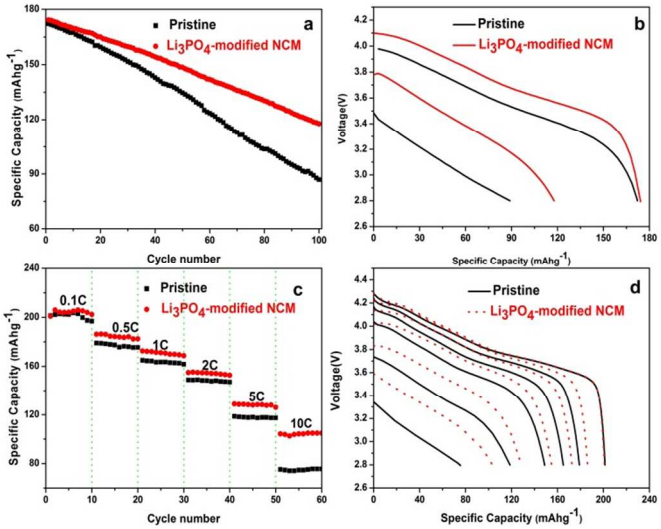


Fig.7 (a) The cycling performance of the electrodes cycled at 2*C* at 60°C, (b) the first and the 100$^{th}$ discharge curves of 2*C* rate. (c) rate capability of electrodes as a function of C rate and (d) the first discharge curves of different *C* rate.

Fig.7(c) shows the rate capability test of the materials from 0.1 to 10*C*. Clearly, $Li_3PO_4$-modified NCM delivers a similar discharge capacity with pristine sample at 0.1*C*. However, as the current density increases, the discharge capacity of pristine NCM decreases rapidly, only 95 mAh·g$^{-1}$ at 10*C*. For the $Li_3PO_4$-modified electrode, it delivers a higher discharge capacity of 137.7 mAh·g$^{-1}$ at 10*C*. The distinct decrease in discharge capacity of pristine NCM is due to the destruction of the surface resulting from the side reactions between the active material and electrolyte. The side reactions will boost the charge transfer resistance after activation. It can be proved in the following EIS tests.

Electrochemical impedance spectroscopic (EIS) analysis (Fig.8(a) and (b)) was carried out in charge state of 4.3 V after the indicated number of 2*C* rate at 60°C. The features are fitted to a circuit model shown in Fig.8(c). The high frequency resistance ($R_{HF}$) corresponds to the combined resistances of a liquid electrolyte, a Li metal anode and an Al foil current collector being ~2-5 Ω for both cells. The first mid-frequency semicircle is attributed to the solid electrolyte interphase resistances ($R_{SEI}$) which occurs at both anode and cathode. The second semicircle observed at lower-frequency ($R_{LF}$) is typically assigned to the interfacial reactions for Li-ion transport on surface of the NCM particles.[24-25] According to the enlarged image in Fig.8 and fitting results in Tab.1, the $R_{SEI}$ values of both samples are small and tend to keep stable as cycle number increases. $R_{LF}$ of both materials increases with cycling and it is notable that the acceleration of pristine electrode is more rapid. After 100 cycles, the $R_{LF}$ value of pristine electrode increases from 68.9 Ω to 834.9 Ω; while the $R_{LF}$ of $Li_3PO_4$-modified electrode is 67.4 Ω after 1 cycle, but only increases to 538.4 Ω after 100 cycles. Increasing $R_{LF}$ during cycling indicates more side reactions resulted from HF and/or unstable $Ni^{4+}$ ions between the active material and electrolyte. In our previous report, we found surface coating is helpful to slow down the side reactions,[13] but the role of $Li_3PO_4$ in

isolating from electrolyte is negligible because of no coating layer. The enhanced battery performance may benefit from no synthetic residues $Li_2O$/LiOH on surfaces during cycling.

Specifically, $LiPF_6$-based electrolyte contains a small amount of water and the existence of water causes breakdown of the electrolyte accompanying by HF generation, as suggested by Aurbach et al. and Edström et al.:[26-27]

$$LiPF_6 \rightarrow LiF\downarrow + PF_5 \quad (2)$$

$$PF_5 + H_2O \rightarrow POF_3 + 2HF \quad (3)$$

$$POF_3 + Li_2O^- \rightarrow LiF\downarrow + Li_xPOF_y \quad (4)$$

That is to say, HF is generated in the electrolyte from the hydrolysis of $LiFP_6$. However, the lithium residues $Li_2O$/LiOH will further accelerate the hydrolysis of $LiFP_6$ and produce more HF, LiF and $Li_xPOF_y$ type compounds as shown above, which are highly resistive to Li migration.[28] Additionally, $Li_2O$/LiOH will react with HF (generated in the electrolyte) and produce more water. Although both $Li_3PO_4$ and LiF are the same as insulating layer, and precipitated $Li_3PO_4$ will react and HF as following $Li_3PO_4$+HF→ LiF+ $Li_2HPO_4$/$LiH_2PO_4$. According to this reaction, it will bring less LiF and no water when compared with the reaction between $Li_2O$/LiOH and HF. Hence the low LiF content formed on the surface of NCM may be responsible for relatively better electrochemical performance of $Li_3PO_4$-modified NCM.

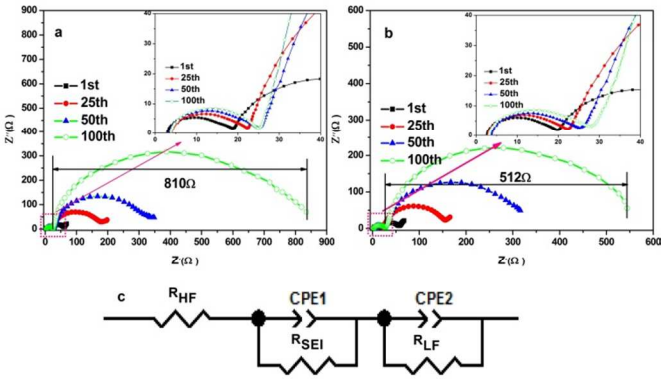


Fig.8 Nyquist plots of pristine (a) and $Li_3PO_4$-modified NCM (b) after different cycling numbers at charge state.

Tab.1 Fitted $R_{HF}$, $R_{SEI}$ and $R_{LF}$ of NCM electrodes at discharge state after various cycling number under 60 ℃

| Cycling number | Pristine NCM | | | $Li_3PO_4$-modified NCM | | |
|---|---|---|---|---|---|---|
| | $R_{HF}$ | $R_{SEI}$ | $R_{LF}$ | $R_{HF}$ | $R_{SEI}$ | $R_{LF}$ |
| 1 cycle | 3.0 | 18.7 | 68.9 | 2.7 | 19.8 | 67.4 |
| 25 cycles | 3.9 | 22.2 | 197.7 | 3.0 | 22.1 | 165.6 |
| 50 cycles | 3.6 | 24.8 | 348.4 | 3.6 | 25.0 | 315.8 |
| 100 cycles | 3.8 | 24.9 | 834.9 | 3.2 | 26.4 | 538.4 |

We have tried to understand the enhanced battery performances of $Li_3PO_4$-modified NCM from the electrolyte and active materials recovered from cycled cells at 60°C. The amount of HF in DMC measured by HF titration is about 233.5 ppm for the pristine NCM and 156.8 ppm for $Li_3PO_4$-modified NCM, which is consistent with above conclusion. Additionally, we make further efforts to obtain the mechanism of the $Li_3PO_4$-modified NCM with XPS, which was used to investigate the surface of cycled electrodes. Before XPS test, the residual electrolyte on all the cycled electrodes was removed by DMC and dried. Fig.9(a and b) depicts the Ni 2p2/3 and F 1s spectra of pristine and $Li_3PO_4$-modified NCM, respectively. The spectra of the cathodes between 859 and 852 eV can be deconvoluted into $Ni^{2+}$ and $Ni^{3+}$ peaks. There is no assignment on the peak at ~858 eV before the cycling. After extensive cycles, both samples display peaks at ~858 eV, although there are intensity variations. According to the handbook of X-ray photoelectron spectroscopy by C.D. Wagner, the peak at ~858 eV is ascribed to the $NiF_2$ and the peak at ~855.2 eV is attributed to $Ni^{3+}$ in bulk. From the relative area ratio of $Ni^{2+}$/$Ni^{3+}$, we can know the cathode material has been protected from erosion after $(NH_4)_2HPO_4$ processed. In this regard, the removal of lithium residues on surface of $LiNiO_2$-based materials is very effective in decreasing the side reactions. This is further illustrated by the F1s peak, which is commonly used to determine the content of LiF on the surfaces of the NCM. As depicted in Fig.9(b) and (d), the peak between 687 and 689 eV is ascribed to PVDF, and the peak around 685.4 eV results from LiF.[27] LiF is a very resistive compound and is expected to cause battery fading when presents on surface of electrode. The $Li_3PO_4$-modified NCM with lower content of $NiF_2$ and LiF on their surfaces are responsible for lower electrode polarization and better electrochemical cycling stability in Fig.7 and Fig.8. This result clearly means that propagation of LiF and HF is greatly suppressed after the removal of lithium impurities.

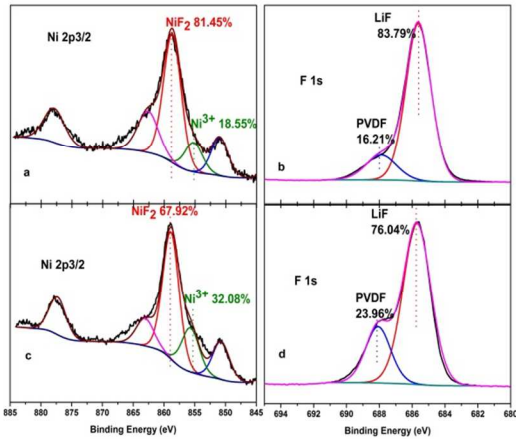


Fig.9 XPS spectra of Ni 2p3/2 and F 1s in pristine (a), (b) and $Li_3PO_4$-modified NCM (c), (d) after 60°C cycling.

## Conclusions

Taking $LiNi_{0.8}Co_{0.1}Mn_{0.1}O_2$ as an example, we have tried to understand the improved battery performance of $Li_3PO_4$-modified $LiNiO_2$-based cathode materials. Although the in-situ precipitated $Li_3PO_4$ is not coated on surface, the results clearly demonstrate that propagation of LiF and HF during cycling is greatly suppressed after the removal of lithium impurities by $(NH_4)_2HPO_4$. The $Li_3PO_4$-modified $LiNi_{0.8}Co_{0.1}Mn_{0.1}O_2$ cell is able to maintain the initial capacity of about 66.9%, whereas that of the pristine sample is only 48.1% during 100 cycles at 60°C. Further work is required to study the storage performance of $Li_3PO_4$-modified $LiNiO_2$-based in air because it can hardly isolate the materials from air.

## *Acknowledgements*

This work was financially supported by the National Basic Research Program of China (2014CB643406) and Hunan Provincial Innovation Foundation For Postgraduate.

## References

1 M.-H. Kim, H.-S. Shin, D. Shin and Y.-K. Sun, *J. Power Sources*, 2006, 159, 1328.

2 Y.-K. Sun, S.T. Myung, B.C. Park, J. Prakash, I. Belharouak and K. Amine, *Nat. Mater.*, 2009,8, 320.
3 J. Shim, R. Kostecki, T. Richardson, X. Song and K.A. Striebel, *J. Power Sources*, 2002, 112, 222.
4 G.V. Zhuang, G. Chen, J. Shim, X. Song, P.N. Ross and T.J. Richardson, *J. Power Sources*, 2004, 134, 293.
5 S. W. Song, G. V. Zhuang and P. N. Ross, *J. Electrochem. Soc*., 2004, 151, A1162.
6 K. Matsumoto, R. Kuzuo, K. Takeya and A. Yamanaka, *J. Power Sources*, 1999, 81/82, 558.
7 K. Shizuka, C. Kiyohara, K. Shima and Y. Takeda, *J. Power Sources*, 2007, 166, 233.
8 H.S. Liu, Z.R. Zhang, Z.L. Gong and Y. Yang, *Electrochem. Solid-State Lett*., 2004, 7(7), A190.
9 A.M. Andersson, D.P. Abraham, R. Haasch, S. MacLaren, J. Liu and K. Amine, *J. Electrochem. Soc*., 2002, 149, A1358.
10 Y. Kim and J. Cho, *J. Electrochem. Soc*., 2007, 154, A495.
11 J. Eom, M.G. Kim and J. Cho, *J. Electrochem. Soc*., 2008, 155, A239.
12 D.-J. Lee, B. Scrosati and Y.-K. Sun, *J. Power Sources*, 2011, 196, 7742.
13 X. H. Xiong, Z. X. Wang, H. J. Guo, Q. Zhang and X. H. Li, *J. Mater. Chem. A*, 2013, 1, 1284.
14 M. Gu, I. Belharouak, A. Genc, Z. G. Wang, D. P. Wang, K. Amine, F. Gao, G. W. Zhou, S. Thevuthasan, D. R. Baer, J.-G. Zhang, N. D. Browning, J. Liu and C. M. Wang, *Nano Lett.*, 2012, 12, 5186.
15 M. Gu, I. Belharouak, J. M. Zheng, H. M. Wu, J. Xiao, A. Genc, K. Amine, S. Thevuthasan, D. R. Baer, J.-G. Zhang, N. D. Browning, J. Liu and C. M. Wang, *ACS Nano*, 2013, 7, 760.
16 M. G. Kim and J. Cho, *J. Mater. Chem.*, 2008, 18, 5880.
17 G. T.-K. Fey, V. Subramanian, J.-G. Chen, *Electrochem. Comm.*, 2001, 3, 234.
18 K. Shizuka, C. Kiyohara, K. Shima, Y. Takeda, *J. Power Sources*, 2007, 166, 233.
19 G.-R. Hu, X.-R. Deng, Z.-D. Peng and K. Du, *Electrochim. Acta*, 2008, 53, 2567.
20 R. Moshtev, P. Zlatilova, S. Vasilev, I. Bakalova and A. Kozawa, *J. Power Sources*, 1999, 81/82, 434.
21 J. Cho, J.-G. Lee, B. Kim, B. Park, *Chem. Mater.,* 2003, 15, 3190.
22 J.-H. Wang, Y. Wang, Y.-Z. Guo, Z.-Y. Ren, C.-W. Liu, *J. Mater. Chem. A*, 2013, 1, 4879.
23 K.S. Tan, M.V. Reddy, G.V.S. Rao and B.V.R. Chowdari, *J. Power Sources*, 2005, 141, 129.
24 Y.-K. Sun, S.-T. Myung, C. S. Yoon and D.-W. Kim, *Electrochem. Solid-State Lett*., 2009, 12, A163.
25 D. Aurbach, J. Electrochem. Soc., 1989, 136, 906.
26 K. Edström, T. Gustafsson, J. O. Thomas and *Electrochim. Acta*, 2004, 50, 397.
27 S. Verdier, L. El Ouatani, R. Dedryvère, F. Bonhomme, P. Biensan and D. Gonbeau, *J. Electrochem. Soc*., 2007, 154(12), A1088.
28 J. M. Zheng, M. Gu, J. Xiao, P. J. Zuo, C. M. Wang and J.-G. Zhang, *Nano Lett.*, 2013, 13, 3824.

## Notes

[a] School of Metallurgy and Environment, Central South University, Changsha 410083, P.R. China.
[b] Department of Materials Science and Engineering, Georgia Institute of Technology, Atlanta, GA 30332-0245, USA
1 These authors contributed equally to this work.